Noname manuscript No.
(will be inserted by the editor)

Automatic Collateral Circulation Scoring in Ischemic Stroke using 4D CT Angiography with Low-Rank and Sparse Matrix Decomposition

Mumu Aktar · Donatella Tampieri · Hassan Rivaz · Marta Kersten-Oertel · Yiming Xiao

Received: date / Accepted: date

Abstract Purpose: Sufficient collateral blood supply is crucial for favorable outcomes with endovascular treatment. The current practice of collateral scoring relies on visual inspection and thus can suffer from inter and intra-rater inconsistency. We present a robust and automatic method to score cerebral collateral blood supply to aid ischemic stroke treatment decision making. The developed method is based on 4D dynamic CT angiography (CTA) and the ASPECTS scoring protocol.

Methods: The proposed method, ACCESS (**A**utomatic **C**ollateral **C**irculation **E**valuation in i**S**chemic **S**troke) estimates a target patient's unfilled cerebrovasculature in contrast-enhanced CTA using the lack of contrast agent due to clotting. To do so, the fast Robust Matrix Completion (fRMC) algorithm with in-face extended Frank-Wolfe optimization is applied on a cohort of healthy subjects and a target patient, to model the patient's unfilled vessels and the estimated full vasculature as sparse and low-rank components respectively. The collateral score is computed as the ratio of the unfilled vessels to the full vasculature, mimicking existing clinical protocols.

Results: ACCESS was tested with 46 stroke patients and obtained an overall accuracy of 84.78%. The optimal threshold selection was evaluated using a receiver operating characteristics (ROC) curve with the leave-one-out approach and a mean area under the curve (AUC) of 85.39% was obtained.

Conclusion: ACCESS automates collateral scoring to mitigate the shortcomings of the standard clinical practice. It is a robust approach, which resembles how radiologists score clinical scans, and can be used to help radiologists in clinical decisions of stroke treatment.

Keywords Ischemic Stroke · Collateral Supply · CT Angiography · Low-rank and Sparse

Mumu Aktar
Computer Science & Software Engineering, Concordia University
1455 boul. De Maisonneuve O.
Montréal (Québec), H3G 1M8, Canada
Tel.: +1 (514) 848-2424 ext.7164
E-mail: m_ktar@encs.concordia.ca

1 Introduction

Stroke is one of the leading causes of disability and death worldwide. Statistics from the World Heart Federation show that each year 15 million people suffer from stroke among which 5 million become permanently disabled and 6 million people die [1]. There are two kinds of stroke: ischemic, where a blood clot forms in a cerebral artery, and hemorrhagic, where a cerebral vessel ruptures and bleeds into the brain. Ischaemic stroke is much more frequent with 8 out of 10 people suffering from it.

When diagnosis and treatment of stroke are not performed in time, patients become disabled due to a lack of blood and oxygen, which causes neuronal cell death in the affected part of the brain. Treatment strategies are chosen based on a number of factors including time window, infarct volume, penumbra size, and collateral circulation. A patient can be treated after 6 hours of symptoms onset with endovascular treatment, where a catheter with a mechanical device attached to the tip is used to remove the clot. This mechanical intervention allows blood flow to quickly be restored. However, not all stroke patients are suitable candidates for endovascular treatment, due to the risks associated with it. One important indication for successful endovascular treatment is the presence of sufficient collateral circulation (i.e., *collaterals*) [6].

Grading the extent of collateral circulation is an important factor for treatment decision making, and a number of approaches have been developed to visually quantify collateral circulation, including ASITN/SIR Collateral Score, Miteff System, Mass System, modified Tan Scale, and ASPECTS (Alberta Stroke Program Early CT Score)[25]. With these approaches, performance depends on the experience, training, and specialty of radiologists, and thus can result in inter- and intra-rater inconsistency which have been shown to be an issue in a number of studies [12] [5] [19]. Grotta *et al.* [12] concluded that it is difficult to get the agreement in recognizing and quantifying early ischemic changes even by experienced clinicians. A recent study by Grunwald *et al.* [13] showed that between individual neuroradiologists, the intraclass correlation coefficient ranges from 0.42 to 0.86 and score agreements range from 36.2% to 81.6%. Automated scoring systems aim to provide robust methods that do not suffer from inter- and intra-rater inconsistencies.

2 Related Work

A number of automatic and semi-automatic methods have been developed to facilitate treatment decisions in ischemic stroke. Kersten-Oertel *et al.* [17] developed a method that considered differences of mean intensities on the left and right hemispheres. The results of this method showed a good correlation ($r^2 = 0.71$) between the radiologist and computed score but the method itself had difficulty dealing with individual variations, e.g. from calcification, as well as, normal vasculature asymmetry between hemispheres. Boers *et al.* [3] also considered the ratio between left and right hemispheres for quantitative measurement of collateral status and obtained a good correlation, ρ of 0.75 ($p < .001$) between visual and quantitative collateral score. In their work, multiscale segmentation was done on baseline

[1] http://www.world-heart-federation.org/cardiovascular-health/stroke/.

CTA with better result for arteriovenous acquisition phase to obtain the vasculature before the collateral evaluation. In the work by Xiao *et al.* [29], support vector machines (SVM) were used to score collateral supply after extracting blood vessels automatically using low-rank decomposition. The results of this method showed good separation between good and intermediate versus poor collaterals with an overall accuracy of 82.2%. The drawback of this machine learning-based method is that performance is affected by limited training data. A random-forest-based classifier was developed by Kuang *et al.* [18], where non-contrast CT (NCCT) was used to automate the ASPECTS assessment. The intra-class correlation coefficient between the automated ASPECTS method and the DWI ASPECTS score by experts was found to be 0.76, but NCCT may not be sensitive enough for those with good collaterals. Shieh *et al.* [27] developed a computer-aided decision system for thrombolysis therapy using NCCT. Their scoring based on a contralateral comparative method is independent of ground truth and obtained an area under the curve (AUC) of 90.2%. Collateral assessment with 4D CTA was performed by Frolich *et al.* [11] using the semi-quantitative regional leptomeningeal collateral score (rLMC), proving that temporally fused maximum intensity projections (tMIPs) can better depict the collateral flow. Their study obtained an inter-rater agreement with an intraclass correlation coefficient of 0.78. However, their experiments were limited to certain time points rather than the entire 4D CTA series and confined to only subjects with good collaterals. Zhang *et al.* [31] have integrated the velocity and extent of collaterals in the peak phase and tMIPs to obtain a collateral grading score (CGS) using 4D CTA. Using the rLMC semi-quantitative approach to set the CGS cutoff, the method resulted in an AUC of 0.80. Table 1 summarizes the main highlights of the existing approaches for collateral grading.

In this paper, we describe an automated image-processing approach ACCESS (**A**utomatic **C**ollateral **C**irculation **E**valuation in i**S**chemic **S**troke) for evaluating collateral circulation with the ASPECTS protocol as the reference, which has been shown to be a reliable, systematic and robust approach. The ASPECTS score is based on the extent of contrast opacification in arteries distal to the occlusion clot [24]. Our goal is to use robust low-rank and sparse decomposition to obtain unenhanced collaterals in a patient from the group behavior of normal controls. The developed model is based on the assumption that from the group of normal controls and one target patient taken as columns in a low-rank matrix completion framework, the unfilled collaterals of a stroke patient can be reconstructed in the sparse component whereas the unchanged full vasculature appears in the low-rank component. Based on this concept, we developed a novel automated approach for collateral scoring which considers the ratio of unenhanced collaterals to the full vasculature and determines the collateral score using this ratio. ACCESS uses the fast robust matrix completion (fRMC) method [26] to extract blood vessels benefiting from the in-face extended Frank-Wolfe algorithm [10], a method for solving a defined convex optimization problem.

3 Materials and Methods

The ACCESS pipeline is shown in Fig. 1 and described in detail in the following section.

Table 1: A brief survey of existing collateral scoring techniques using CTA.

Ref	**Data**	**Scoring**	**Cases**	**Method and Results**
Shieh *et al.*[27]	NCCT	ASPECTS	103	Contralateral automatic comparative method; AUC of 90.2%
Frolich *et al.*[11]	4D CTA	rLMC	82	Manual grading; tMIP best for collateral prediction; intra-class correlation of 0.78
Zhang *et al.* [31]	4D CTA	rLMC	80	CGS used by combining velocity & extent of collaterals; AUC of 0.80
Kersten *et al.*[17]	4D CTA	ASPECTS	29	Intensity differences between left & right hemisphere; Correlation of method to radiologist had $r^2 = 0.71$
Xiao *et al.*[29]	4D CTA	ASPECTS	37	Machine learning method based on SVM; Overall accuracy of 82.2%
Kuang *et al.*[18]	NCCT	ASPECTS	257	Random forest based classifier; Intra-class correlation coefficient between proposed method & experts was 0.76
Boers *et al.*[3]	CTA	Tan System [28]	422	Vascular ratio between left & right hemispheres; Correlation of 0.75 between visual and quantitative score
Grunwald *et al.*[13]	CTA	Tan System [28]	98	Automated e-CTA score; 90% agreement with radiologist, intra-class correlation coefficient of 0.93
ACCESS (Proposed method)	4D CTA	ASPECTS	54	Automatic collateral circulation scoring; An average AUC of 85.39%

3.1 Scanning protocol

Eight healthy subjects were used as reference scans, and 46 subjects with ischemic stroke were used to evaluate our method. All subjects underwent imaging at the Montreal Neurological Hospital (Montreal, Canada). The 4D CTA images were captured on a Toshiba's Aquilion ONE 320-row detector 640-slice cone-beam CT (Toshiba medical systems, Tokyo, Japan). The scanner provides whole-brain perfusion and dynamic vasculature information in one single examination with a single rotation of the gantry. The routine stroke protocol performs a series of intermittent volume scans over a period of 60 seconds with a scanning speed of 0.75 s/rotation. A total of 19 volumes are captured for each patient with low-dose scanning for every 2s during the arterial phase and 5s during the venous phase. Isovue-370 (Iopamidol) was used as a non-ionic and low osmolar contrast medium (Iodine content, 370 mg/ml).

3.2 Pre-processing

Prior to evaluating collateral supply for each stroke patient, we followed a number of pre-processing steps to: (1) register all the subjects (healthy and with stroke) to a standard template space, (2) extract blood vessels (3) refine group-wise blood vessel alignment and (4) enhance vessels using probabilistic segmentation.

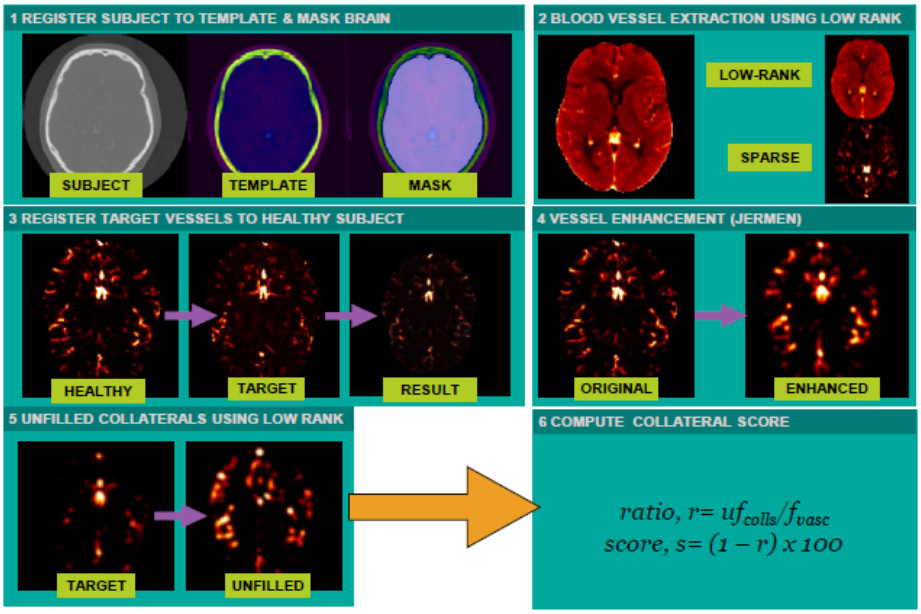

Fig. 1. The overall workflow of the ACCESS method.

3.2.1 Image Registration

To process all the subjects in the same space we performed image registration in two stages. In the first stage, all 18 CTA volumes of an individual subject are rigidly registered to that of the first time point. Next, the first volume is registered non-linearly to a CTA brain template using the symmetric image normalization method (SyN) [2] from ANTs (Advanced Normalization Tools)[2]. Then, the non-linear transformation is applied to all other volumes of that subject. Thus all subject volumes are registered first to each other and then to the template. The CTA brain template was created following the unbiased group-wise registration approach [9] using 12 healthy subjects' brains. A brain mask was created from the template using active contour segmentation in ITK-SNAP (www.itksnap.org) and used to remove the skull of all subjects for further analysis. In the second registration stage, we further refine the vessel alignment, in order to estimate the unfilled blood vessels in the patient through low-rank and sparse decomposition. Therefore, additional nonlinear registration using SyN is performed in this stage between a randomly selected healthy subject's temporal 3D average taken as template and the rest of the 3D subjects participated in further experiments. Note that the temporal 3D average of each subject (averaging along multiple time points) for vessel alignment is obtained after blood vessel extraction described in Section 3.2.2.

[2] stnava.github.io/ANTs

3.2.2 Blood Vessel Extraction

To evaluate collaterals, it is necessary to determine how blood flows over time for each subject. Thus, the static background with grey and white matter, as well as, any calcification, which can affect the scoring are not considered. Similar to the approach proposed by Xiao *et al.* [29], the flow of the contrast agent in the blood vessels are separated from the static background with calcification. However, rather than using the augmented Lagrange multiplier method by Lin *et al.* [21] to recover low-rank and sparse components, we use the more robust fRMC method [26]. This method does not require any parameter tuning and converges very quickly [1] whereas [21] is sensitive to parameter tuning and has a slower convergence rate. For applying low-rank decomposition to a 4D CTA scan, a matrix, $D = [C_s^1, C_s^2, \ldots..C_s^{19}]$ is considered with all the volumes taken as columns of the matrix. The low-rank representation is as below:

$$\min \quad rank(B) \text{ s.t.} \quad D = B + V \tag{1}$$

The minimization of ranks of background, B as in equation (1) for separating the correlated and static background features from the dynamic blood vessels, V is performed by,

$$\min \|B - D\|_F^2 \quad \text{s.t.} \quad \|B\|_* < \delta \tag{2}$$

where $\|.\|_F$ indicates the Frobenius norm, $\|.\|_*$ represents the nuclear norm of a matrix and δ is the constraining upper bound for the nuclear norm of low-rank matrix, B. We can see from Equation 2 that there is no tunable parameter to obtain the low-rank and sparse matrix for fRMC. Since D is a large non-singular matrix with multiple volumes as columns, the square of its Frobenius norm is greater than both its nuclear norm and the nuclear norm of its component, B. Therefore, δ can be comfortably set to any value greater or equal to the square of the Frobenius norm of D. Similar to the study of Ashikuzzaman *et al.* [1] and the reference study of fRMC by Rezaei *et al.* [26] for background subtraction, we set it to ten times the Frobenius norm of D. Thus, we do not need to set any parameters manually for extracting blood vessels and further unfilled collaterals using fRMC. The rank minimization in fRMC is solved using the extended Frank-Wolfe optimizer [10] which requires a lower number of iterations and less computation in each iteration that makes the fRMC method fast. The choice of its convergence parameters, γ_1 and γ_2 mostly affect the convergence speed and rank of the matrix with $0 \leq \gamma_1 \leq \gamma_2 \leq 1$ [26]. We provide further insight of these parameters in Section 5. Finally, we extracted the sparse matrix containing blood vessels by subtracting the background from the original data matrix. The columns obtained in the sparse matrix represent the blood flow in each volume over time. Given this, we can then take the average of the 19 volumes containing blood flow over time to perform collateral scoring in 3D.

3.2.3 Enhancement of Vascular Structures

Vessel enhancement is an important prerequisite for computer-aided clinical procedures to highlight the blood vessels and suppress noise and other non-vascular structures. There is much literature on vessel segmentation. Here, we review a few

recent techniques, but interested readers can refer to [23]. Yang *et al.* [30] developed a vessel segmentation technique following contrast enhancement, boundary refinement, and content-aware regions of interest adjustment by checking shape consistency and connectivity. Rather than considering a region-based method that may be sensitive to unnatural intensity variations, Meijs *et al.* [22] segmented full cerebral vasculatures in 4D CT using weighted temporal variance and local histogram features as inputs to a random forest classifier and obtained an overall accuracy of 0.995. Vessel segmentation by Jin *et al.* [16] utilized the low-rank and sparse decomposition technique to segment vessels from group behavior of the sequence of XCA images and further removed spatially varying noisy residuals through local-to-global adaptive threshold filtering.

In our approach, we used the vessel enhancement by Jermen *et al.* [15] to increase the visibility of the blood vessels in MIPs as well as to make the contrast agent response uniform. This enhancement method outperforms traditional vesselness filtering approaches by enhancing rounded structures along with elongated ones. The filter allows local structures to be distinguished by analyzing the eigenvalues of the Hessian matrix at each point in the image. Let, $\lambda_i, i = 1, 2, 3$ denote the three eigenvalues of the Hessian matrix of a 3D image with the ideal eigenvalue relationship $\lambda_2 \approx \lambda_3 \wedge |\lambda_{2,3}| >> |\lambda_1|$. This relation, however, can't be maintained if the magnitudes of λ_2, λ_3 are very low. So, to ensure robustness in case of lower eigenvalues, a regularization on the value of λ_3 at multiple scales is done by:

$$\lambda_\rho(s) = \begin{cases} \lambda_3 & \text{if} \quad \lambda_3 > \tau max_x \lambda_3(x, s), \\ \tau max_x \lambda_3(x, s) & \text{if} \quad 0 < \lambda_3 \leq \tau max_x \lambda_3(x, s), \\ 0 & \text{otherwise} \end{cases}$$

where s is the vessel scale and τ is the cutoff threshold (value between 0 to 1), which results in a uniform response. Finally, the elliptic cross-section structures are confined to the ratio $\lambda_2 \geq \lambda_\rho/2 > 0$ and the vessel enhancement function is defined as:

$$V_p = \begin{cases} 0 & \text{if} \lambda_2 \leq 0 \vee \lambda_\rho \leq 0, \\ 1 & \text{if} \lambda_2 \geq \lambda_\rho/2 > 0, \\ \lambda_2^2(\lambda_\rho - \lambda_2)\left[\frac{3}{\lambda_2 + \lambda_\rho}\right]^3 & \text{otherwise} \end{cases}$$

V_p can be computed for both bright and dark structures and the filter response is between 0 and 1 but ideally 0 for non-vascular and 1 for vascular structures.

Using this vessel enhancement method, we segmented vessels in all subjects before using them to estimate unfilled collaterals via the second low-rank and sparse decomposition.

3.3 Collateral Circulation Evaluation

For evaluating collateral circulation, the score is categorized into three types: good, intermediate and poor. These scores are defined based on the collateral supply in the occluded MCA territory according to ASPECTS [24]. The ASPECTS score, which we used as ground truth in our experiments, is based on the agreement of the visual assessment of the acquired 4D CTA scans by two radiologists. A score

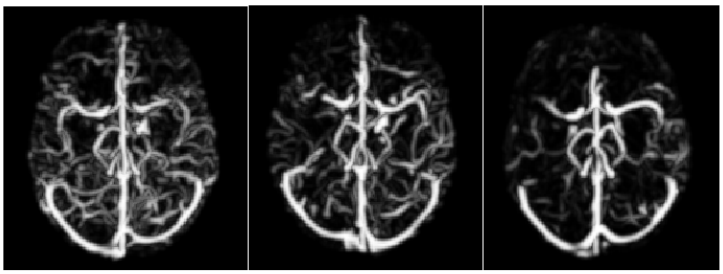

Fig. 2. Example MIP CTAs of different collateral circulation scores.

of good means 100% collaterals, intermediate means greater than 50% and lower than 100% and poor means below 50% and greater than zero (Fig. 2). Since fRMC uses an optimizer to minimize the rank, more variability between individuals can affect the results. To mitigate individual variability, we blurred the data with a Gaussian kernel ($\sigma = 2mm$). Among our 54 subjects, we had 8 normal controls, 14 poor, 17 intermediate, and 15 good subjects.

To measure collateral supply, we compare filled vessels (by contrast agent) with unfilled ones. To obtain the unfilled vessels in a patient, a group of 8 normal subjects and a target subject is created. Normal subjects are considered as healthy with 100% collateral supply. The target collateral score can then be defined using the normal controls. We used the same robust approach fRMC with extended Frank-Wolfe solver in order to obtain the unfilled vessels of a target case into a sparse matrix from the group behavior. Since all the normal controls contain very similar vasculature, the full vasculature is obtained into the low-rank matrix. The data matrix here is defined as, $D = [C_s^1, C_s^2, \ldots..C_s^8, C_s^9]$ where columns, C_s^1 to C_s^8 are the normal subjects and C_s^9 is the test case. Next, low-rank minimization is performed as in Equation (2) which is defined here as:

$$\min \quad \|f\_vasc - D\|_F^2 \quad \text{s.t.} \quad \|f\_vasc\|_* < \delta \tag{3}$$

where f_vasc stands for full vasculature from where we obtain the unfilled collaterals by, uf_colls=D-f_vasc. Finally, the collateral score is measured as below:

$$Ratio, r = uf\_colls/f\_vasc \tag{4}$$

and collateral score in the target subject,

$$Score, s = (1–r) \quad \times \quad 100. \tag{5}$$

4 Experimental Results

4.1 Blood Vessel Extraction

To overcome the inter-volume intensity differences within a scan session, the intensity profiles of all the volumes of a subject are normalized (using Minmax) with respect to the first volume. The fRMC approach is then applied to separate blood

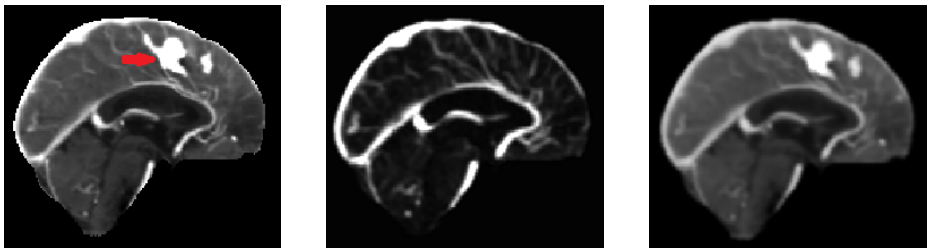

Fig. 3. Example of low-rank decomposition. *Left:* original sagittal view of a subject (red arrow points to a calcification). *Middle:* sparse image containing blood vessels. *Right:* low-rank image with calcification.

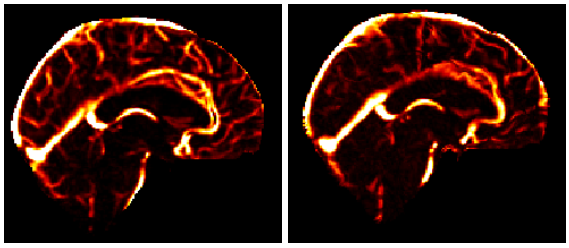

Fig. 4. *Left:* a healthy subject used as a reference image. *Right:* an individual registered to the reference image.

vessels from the background which results in the removal of any calcification (e.g. Fig. 3).

4.2 Image Registration

A two-stage registration was performed by Huck *et al.* [14] to create a cerebral vascular atlas, which used standard parameters from the ANTs tool to align segmented vessels in fine details. Similar to their work, we found that the standard parameters for the SyN algorithm from ANTs worked well for registration to the template as well as the alignment of blood vessels. To align the blood vessels, a SyN deformation on 4 scale levels was done (with iterations of 100x100x50x20). We evaluated the alignment by checking the overlap of blood vessels in multiple subjects extracted by applying low-rank and sparse decomposition. Areas with fewer than 40 connected pixels were ignored to avoid the smallest vessels, which are quite different in each individual and can cause scoring error. The registration performance of an individual subject's blood vessel to a healthy subject is shown in Fig. 4.

4.3 Vessel Enhancement

The blood vessels of an example subject segmented by scaling responses between 0 to 1 using Jermen vessel enhancement function [15] is shown below in (Fig. 5). The

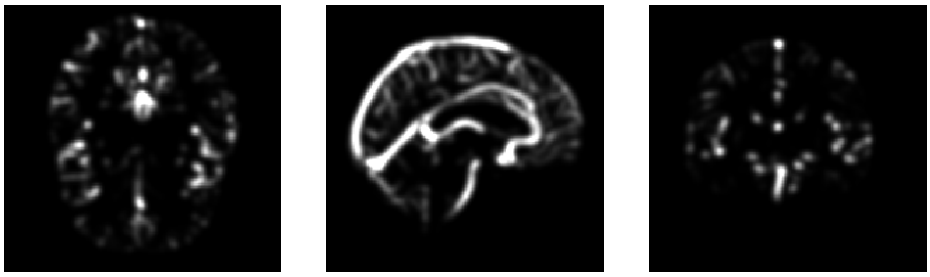

Fig. 5. Vessel enhancement of a subject (axial, sagittal and coronal view).

scale, s, ranging from 0.5mm to 2.5mm with a 0.5mm interval was chosen based on the work of Jermen *et al.* [15] on 3D DSA cerebral vasculature segmentation. The regularization parameter, τ , is varied over the chosen scales from 0.5 to 1 to show the effect on the segmentation outcome in Section 4.5; τ= 0.5 resulted in a uniform response in our dataset.

4.4 Automatic Collateral Circulation Evaluation

To reduce computational complexity and for better visibility, the 2D MIP of the sparse and low-rank matrices in axial directions were taken. Demonstration of low-rank matrix completion to obtain the unfilled vessels in an individual with respect to the cohort of normal subjects is shown in Fig. 6.

From the sparse images, we can see that there are a lot of unenhanced vessels obtained. This is due to the variability of the small vessels in individual subjects which appear as changes in the sparse matrix. Post-processing is performed with thresholding in order to ignore the small vessels' variability, as well as some unwanted portions obtained in the sparse component due to contrast variations. To remove very small vessels, all connected components with fewer than 40 pixels were removed from the binary images obtained by thresholding. To overcome the effect of manual thresholding and make ACCESS more robust, we performed a sensitivity analysis in Section 4.5 to obtain this optimal threshold. Furthermore, the main sinus and arteries are removed before collateral scoring.

The images in Fig. 7 show the binary of the sparse and low-rank components after thresholding.

Finally the collateral score is calculated according to the formula of Equations 4 and 5 using the optimal parameters obtained by the sensitivity analysis. Since there is variability between vessels of individual subjects, which cannot be registered perfectly and the final operation is performed on 2D, the radiologists' scores can be conflicting to use here directly. Thus the scoring performance of ACCESS was evaluated after determining the optimal threshold for each class by computing ROC curves [7] (Fig. 8). A ROC curve is drawn with the experimental scores and the true class labels. The sensitivity and specificity for different threshold settings, which are varied between 0-100, based on the scores were calculated. Choosing for the optimal points on the curve for the thresholds to define the good, intermediate and poor collaterals, we found scores under 55.45% should be considered as poor, between 55.45 and 70.5% intermediate and above 70.5% good. To overcome the

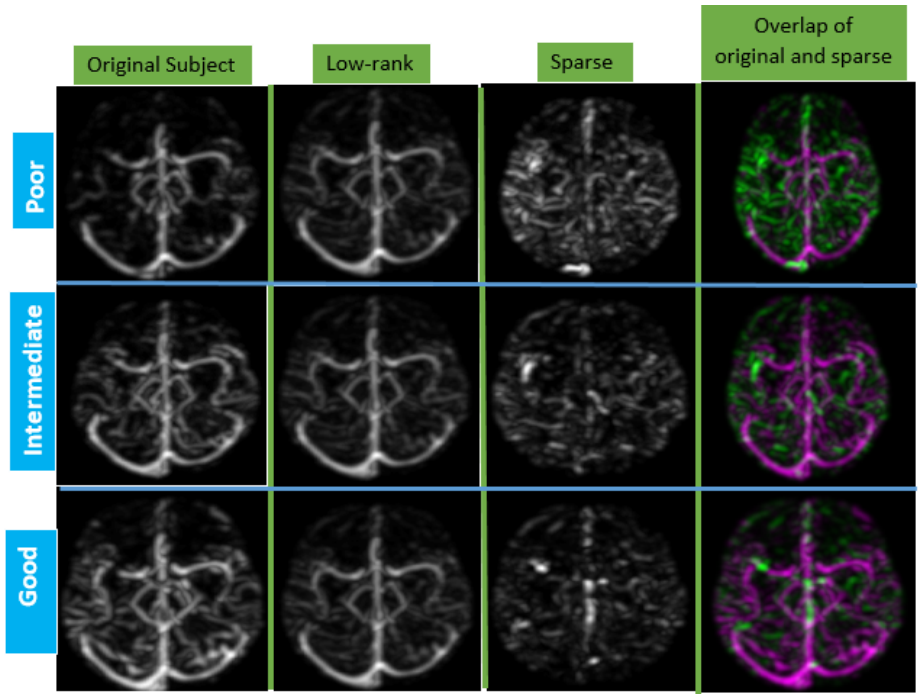

Fig. 6. 2D MIP representation for Low-rank and sparse decomposition for a poor, intermediate and good subject. The overlaid image is shown for better visibility of unfilled vessels (green) with the original collaterals (pink).

effect of over-estimation, we performed a leave-one-out approach to draw the ROC curves and the final curve is drawn from the average of 46 iterations of true positive and false positive rates. An AUC of 85.39% was obtained from the ROC, with AUC of 90.95%, 83.53% and 81.70% for good, intermediate and poor classes respectively. Table 2 shows the confusion matrix. An overall accuracy of 84.78% is obtained from the true positive and true negative results.

Table 2: Confusion Matrix showing ACCESS Results.

Radiologist score / Automatic score	Good	Intermediate	Poor
Good	13	2	0
Intermediate	1	14	2
Poor	1	1	12

4.5 Sensitivity Analysis

In this section, we perform sensitivity analysis for our pipeline on parameter choices of vessel enhancement. Since we do not have any ground truth data for direct

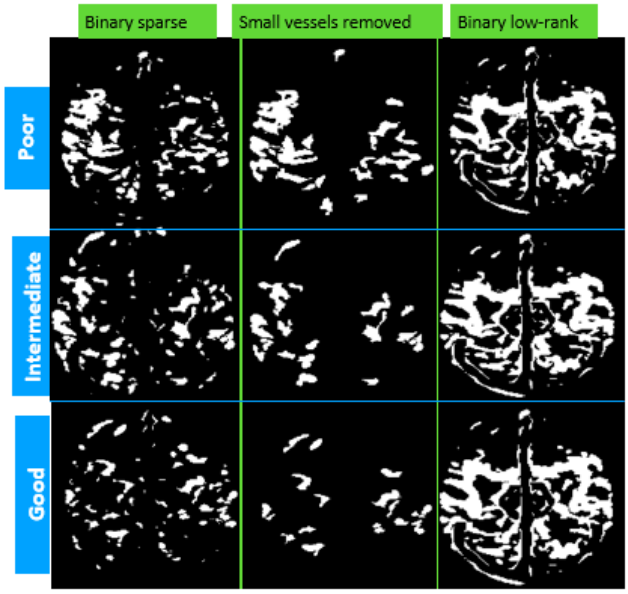

Fig. 7. Post-processing results of 2D MIP of poor, intermediate and good collaterals.

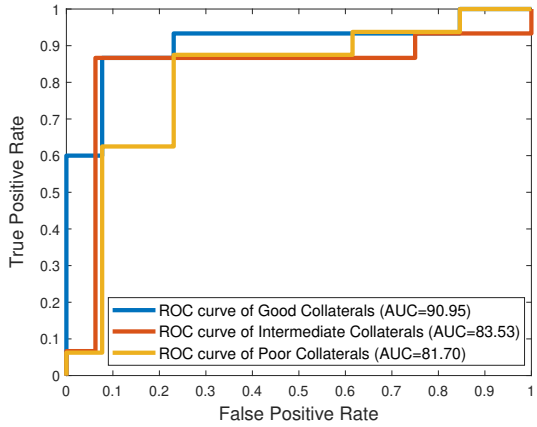

Fig. 8. ROC curves for Good, Intermediate and Poor Collateral Scores Evaluation.

segmentation performance analysis, we assessed the impact of parameters in vessel enhancement (regularization parameter, τ and thresholding value) on the overall performance of ACCESS. The reference study by Jermen's enhancement filtering [15] has shown that probabilistic segmentation of blood vessels can be obtained by setting τ to a value between 0.5 to 1 for a uniform response. Therefore, we tested the scoring results for multiple τ values. We achieved the best result for τ=0.5. In every experiment with different τ, we varied the threshold value within 0.01 to

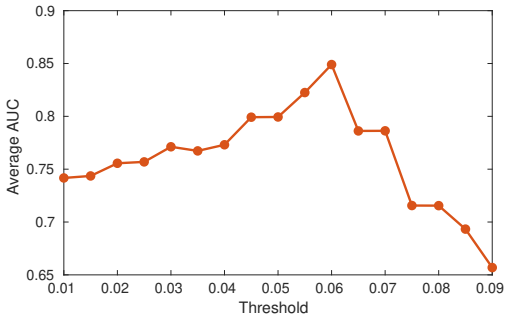

Fig. 9. Average AUC of three classes for varying threshold values.

0.09 (chosen based on the mean intensity of low-rank and sparse images) to obtain the best sensitivity and specificity with the highest AUC in the ROC. Table 3 shows the AUC for each τ with the optimum threshold value.

Table 3: Influence of τ on the Final Evaluation.

τ	**AUC Good**	**AUC Intermediate**	**AUC Poor**	**AUC Average**
0.5	0.909	0.823	0.816	0.849
0.6	0.875	0.798	0.839	0.837
0.7	0.914	0.656	0.843	0.804
0.8	0.909	0.641	0.843	0.798
0.9	0.923	0.637	0.816	0.792
1	0.904	0.660	0.825	0.797

Since τ=0.5 shows the best performance, we achieved the segmentation with this value. Fig. 9 shows how the scoring is sensitive to the varied threshold values. Note that the final ROC curve shown in Fig. 8 from the cross-validation results is done using the optimum threshold value.

4.6 Inter and Intra-rater Variability Analysis

A subset of 27 test cases from the data were rated individually by the two separate radiologists. To show the effect of visual inspection and human rater's variability, we used the consensus ground truth and the separate ratings by the radiologists as well as one of the authors (MA), who served as the third independent rater. The rating is performed based on ASPECTS by assessing the degree of collaterals visually. The subjects' collaterals are scored as "good" if both sides have equal extent of collaterals in any of the phases from arterial to venous with contrast. The same criteria are followed for intermediate and poor subjects with medium and very low extent of collaterals in the affected side of MCA territory compared to the healthy side respectively. To evaluate the inter-rater variability of the two radiologists and the author in the subset of 27 cases, we computed Fleiss' Kappa (κ) statistics [8], which ranges between 0 and 1, (with values from 0.0 to 0.2 indicating slight agreement, 0.21 to 0.40 indicating fair agreement, 0.41 to 0.60 indicating moderate agreement, 0.61 to 0.80 indicating substantial agreement, and

0.81 to 1.0 indicating almost perfect or perfect agreement based on the guidelines of Landis *et al.* [20]) for three raters. With an overall κ=0.455 ($p < 0.0005$), the result represents moderate strength of agreement among the raters. The two radiologists' rating variability on the same subset of cases is obtained by computing a paired Cohen's kappa (κ) statistics [4], yielding κ=0.471 ($p < 0.001$). It should be noted that the collateral score influences the clinical outcome significantly. For example, a "poor" case misclassified as being "good" can cause excessive bleeding leading to hemorrhagic stroke with EVT while a "good" case being misclassified as "poor" ignores a patient from EVT. Due to the raters' variability, poor treatment decisions might be made, which would adversely impact patients. In the subset, the two radiologists have disagreement in scoring poor vs. intermediate in 10% of cases, 11% for poor vs. good and 35% for good vs. intermediate cases. These findings (56% of cases misclassified) fall in the middle of the range of what Grunwald *et al.* [13] found where score agreements range from 36.2% to 81.6%. Further, to show the agreement between ACCESS and radiologists' scores, we computed Cohen's kappa [4] with κ=0.771 ($p < .0005$) and obtained a substantial agreement between the automated approach and radiologists' score. To verify the scoring quality of the independent rater (MA), we computed Cohen's kappa coefficient [4] between the independent rater and the consensus of two expert raters and obtained a substantial agreement with κ=0.649 ($p < 0.0005$). Finally, to assess intra-rater variability, two separate ratings were performed with an interval of 5 days by the same rater MA to compute kappa statistics with κ=0.530 ($p < 0.0005$). Based on the statistics, we can see how the inter- and intra-rater variability between human raters potentially affect the collateral scoring.

4.7 Computation Times

Processing was done on a Windows 7 machine equipped with an Intel(R) Core(TM) i7-4770 CPU @ 3.40GHz and 28 GB of RAM. Registration using ANTS took an average of 19 minutes to register an individual to the template and a further 16 minutes for vessel alignment. The other processing steps are faster, calcification removal takes under 2 minutes, vessel enhancement for individual 3D scans takes 10 seconds and the overall scoring from the sequence of 8 patients is completed within 25 seconds. In order to reduce the processing time of registration, in the future, we will port the pipeline to the GPU.

5 Discussion and Future Work

The novelty of ACCESS is using the group behavior of normal controls to score the collaterals in ischemic stroke patients. We used the robust fRMC approach to obtain the sparsity and low-rank metrics of blood vessels in 4D CTA. Most previous methods used other imaging techniques or didn't consider the fRMC approach to score collaterals, and thus direct comparisons with the state-of-the-art methods are beyond the scope of the paper.

Our proposed method has several advantages over previous techniques. First, very few automated techniques rely on 4D CTA which gives detailed and dynamic

filling information of collaterals. The *automatic* approaches that do exist for collateral supply evaluation use single-phase CTA, which may result in inaccurate estimation of collaterals due to suboptimal selection of a time point for scanning. Second, our approach is less dependent on feature selection and training data, potentially making it more robust in practice. Specifically, machine learning-based automatic approaches can be reliable only when there is a large dataset to overcome overfitting. In contrast, the developed ACCESS method is reliable as it is less independent of training. Thus not only does our method take advantage of full dynamic flow information from 4D CTA but it is also automatic and yields results inline or better than previous methods. Furthermore, the assessment of the final score resembles the definition of collateral circulation status, which is more intuitive for the physicians to employ.

Experiments as well as existing studies [14] have proved that the reference parameters from the state-of-the-art medical imaging registration toolkit, ANTs, used in the registration blocks of the pipeline are robust for our applications (i.e., registration to the template and fine alignment of vessels). To test the impact of vessel segmentation parameters and the threshold used in post-processing, a sensitivity analysis was performed to obtain the optimal parameters for final evaluation. Based on the optimal parameters, collateral grading performance is analyzed using a ROC curve to find cutoffs for scores from different cutoff value settings in a leave-one-out approach. The experimental design of parameter choices with best sensitivity and specificity gives the satisfactory AUC for scoring collateral circulation. This also makes our method more robust.

As noted previously, fRMC is independent of tunable parameters. To assess the impacts of the convergence parameters, γ_1 and γ_2 in the extended Frank-Wolfe optimizer, we evaluate the performance of ACCESS varying γ_1 and γ_2 in the step size of 0.1 following the range of $0 \leq \gamma_1 \leq \gamma_2 \leq 1$ with best τ obtained from previous sensitivity analysis. It can be seen in Fig. 10 that ACCESS performance in terms of AUC is fairly stable across different γ_1 and γ_2. Note that when only γ_1 is set to 0, the AUC decreases slightly (from 0.85 to 0.81).

Although our method doesn't require many data for the evaluation, in the future, the cohort of normal subjects can be enriched for better performance. A more thorough validation of ACCESS is still needed, with a larger dataset from different CT scanners and acquisition protocols, and this will be explored in future work.

The extent of collaterals in intermediate and good subjects were very similar in some cases. Since inter- and intra-rater variability still remains for scoring those subjects, we will seek further validation of our method with ground truth labels collected from consensus of more raters to improve data annotation quality.

6 Conclusion

In this paper, we proposed the ACCESS method for automatic scoring of collateral circulation in the context of treatment decision making in ischemic stroke. To the best of our knowledge, it is the first approach with low-rank and sparse decomposition for collateral score evaluation in ischemic stroke using 4D CTA. With an analogue to existing collateral scoring protocols and being less reliant on machine learning methods that require large amounts of training data, the approach may

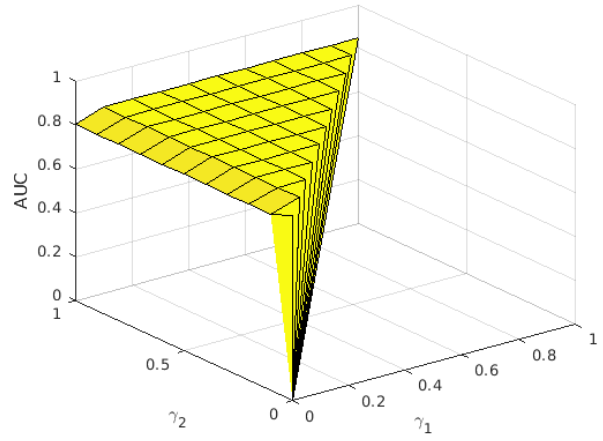

Fig. 10. Demonstration of γ_1 and γ_2 choices on AUC of the overall system.

be more robust than human-rater scoring and more easily comprehensible in the clinical environment.

Acknowledgements This study was funded by NSERC Discovery Grant RGPIN 04136 and Fonds de recherche du Quebec – Nature et technologies (FRQNT Grant F01296). The author Y. Xiao is supported by BrainsCAN and CIHR fellowships. We would like to thank Dr. Ali Alamer and Dr. Johanna Ortiz Jimenez for facilitating data acquisition and annotation.

Ethical approval, Informed Consent and Conflict of Interest

All procedures performed in studies involving human participants were in accordance with the ethical standards of the University Human Research Ethics Committee. Informed consent was obtained from all participants included in the study. The authors declare that they have no conflict of interest.

References

1. Ashikuzzaman M, Belasso C, Kibria MG, Bergdahl A, Gauthier CJ, Rivaz H (2019) Low rank and sparse decomposition of ultrasound color flow images for suppressing clutter in real-time. IEEE Transactions on Medical Imaging
2. Avants BB, Epstein CL, Grossman M, Gee JC (2008) Symmetric diffeomorphic image registration with cross-correlation: evaluating automated labeling of elderly and neurodegenerative brain. Medical image analysis 12(1):26–41
3. Boers A, Barros RS, Jansen I, Berkhemer O, Beenen L, Menon BK, Dippel D, van der Lugt A, van Zwam W, Roos Y, van Oostenbrugge RJ (2018) Value of quantitative collateral scoring on ct angiography in patients with acute ischemic stroke. American Journal of Neuroradiology 39(6):1074–1082

4. Cohen J (1960) A coefficient of agreement for nominal scales. Educational and psychological measurement 20(1):37–46
5. Coutts SB, Hill MD, Demchuk AM, Barber PA, Pexman J, Buchan A, Mak H, Yau K, Chan B (2003) Aspects reading requires training and experience. Stroke 34(10):e179
6. Cuccione E, Padovano G, Versace A, Ferrarese C, Beretta S (2016) Cerebral collateral circulation in experimental ischemic stroke. Experimental & translational stroke medicine DOI 10.1186/s13231-016-0015-0
7. Fawcett T (2006) An introduction to roc analysis. Pattern recognition letters 27(8):861–874
8. Fleiss JL (1971) Measuring nominal scale agreement among many raters. Psychological bulletin 76(5):378
9. Fonov V, Evans AC, Botteron K, Almli CR, McKinstry RC, Collins DL, Group BDC (2011) Unbiased average age-appropriate atlases for pediatric studies. Neuroimage 54(1):313–327
10. Freund RM, Grigas P, Mazumder R (2017) An extended frank–wolfe method with "in-face" directions, and its application to low-rank matrix completion. SIAM Journal on Optimization 27(1):319–346
11. Frolich AM, Wolff SL, Psychogios MN, Klotz E, Schramm R, Wasser K, Knauth M, Schramm P (2014) Time-resolved assessment of collateral flow using 4d ct angiography in large-vessel occlusion stroke. European radiology 24(2):390–396
12. Grotta JC, Chiu D, Lu M, Patel S, Levine SR, Tilley BC, Brott TG, HaleyJr EC, Lyden PD, Kothari R, Franke M, Lewandowski CA, Libman R, Kwiatkowski T, Broderick JP, Marler JR, Corrigan J, Huff S, Mitsias P, Talati S, Tanne D (1999) Agreement and variability in the interpretation of early ct changes in stroke patients qualifying for intravenous rtpa therapy. Stroke 30(8):1528–1533
13. Grunwald IQ, Kulikovski J, Reith W, Gerry S, Namias R, Politi M, Papanagiotou P, Essig M, Mathur S, Joly O, Hussain K, Wagner V, Shah S, Harston G, Vlahovic J, Walter S, Podlasek A, Fassbenderh K (2019) Collateral automation for triage in stroke: Evaluating automated scoring of collaterals in acute stroke on computed tomography scans. Cerebrovascular Diseases 47(5-6):217–222
14. Huck J, Wanner Y, Fan AP, Jäger AT, Grahl S, Schneider U, Villringer A, Steele CJ, Tardif CL, Bazin PL, Gauthier CJ (2019) High resolution atlas of the venous brain vasculature from 7 t quantitative susceptibility maps. Brain Structure and Function 224(7):2467–2485
15. Jerman T, Pernuš F, Likar B, Špiclin Ž (2016) Enhancement of vascular structures in 3d and 2d angiographic images. IEEE transactions on medical imaging 35(9):2107–2118
16. Jin M, Hao D, Ding S, Qin B (2018) Low-rank and sparse decomposition with spatially adaptive filtering for sequential segmentation of 2d+ t vessels. Physics in Medicine & Biology 63(17):17LT01
17. Kersten-Oertel M, Alamer A, Fonov V, Lo B, Tampieri D, Collins L (2016) Towards a computed collateral circulation score in ischemic stroke. arXiv preprint arXiv:200107169
18. Kuang H, Najm M, Chakraborty D, Maraj N, Sohn SI, Goyal M, Hill M, Demchuk A, Menon B, Qiu W (2018) Automated aspects on non-contrast

ct scans in acute ischemic stroke patients using machine learning. American Journal of Neuroradiology DOI 10.3174/ajnr.A5889
19. von Kummer R, Holle R, Gizyska U, Hofmann E, Jansen O, Petersen D, Schumacher M, Sartor K (1996) Interobserver agreement in assessing early ct signs of middle cerebral artery infarction. American journal of neuroradiology 17(9):1743–1748
20. Landis JR, Koch GG (1977) The measurement of observer agreement for categorical data. biometrics pp 159–174
21. Lin Z, Chen M, Ma Y (2010) The augmented lagrange multiplier method for exact recovery of corrupted low-rank matrices. arXiv preprint arXiv:10095055
22. Meijs M, Patel A, van de Leemput SC, Prokop M, van Dijk EJ, de Leeuw FE, Meijer FJ, van Ginneken B, Manniesing R (2017) Robust segmentation of the full cerebral vasculature in 4d ct of suspected stroke patients. Scientific reports 7(1):1–12
23. Moccia S, De Momi E, El Hadji S, Mattos LS (2018) Blood vessel segmentation algorithms—review of methods, datasets and evaluation metrics. Computer methods and programs in biomedicine 158:71–91
24. Pexman JW, Barber PA, Hill MD, Sevick RJ, Demchuk AM, Hudon ME, Hu WY, Buchan AM (2001) Use of the alberta stroke program early ct score (aspects) for assessing ct scans in patients with acute stroke. American Journal of Neuroradiology 22(8):1534–1542
25. Piedade GS, Schirmer CM, Goren O, Zhang H, Aghajanian A, Faber JE, Griessenauer CJ (2019) Cerebral collateral circulation: a review in the context of ischemic stroke and mechanical thrombectomy. World neurosurgery 122:33–42
26. Rezaei B, Ostadabbas S (2017) Background subtraction via fast robust matrix completion. In: Proceedings of the IEEE International Conference on Computer Vision, pp 1871–1879
27. Shieh Y, Chang CH, Shieh M, Lee TH, Chang YJ, Wong HF, Chin SC, Goodwin S (2014) Computer-aided diagnosis of hyperacute stroke with thrombolysis decision support using a contralateral comparative method of ct image analysis. Journal of digital imaging 27(3):392–406
28. Tan I, Demchuk A, Hopyan J, Zhang L, Gladstone D, Wong K, Martin M, Symons S, Fox A, Aviv R (2009) Ct angiography clot burden score and collateral score: correlation with clinical and radiologic outcomes in acute middle cerebral artery infarct. American Journal of Neuroradiology 30(3):525–531
29. Xiao Y, Alamer A, Fonov V, Lo BW, Tampieri D, Collins DL, Rivaz H, Kersten-Oertel M (2017) Towards automatic collateral circulation score evaluation in ischemic stroke using image decompositions and support vector machines. In: Molecular Imaging, Reconstruction and Analysis of Moving Body Organs, and Stroke Imaging and Treatment, Springer, pp 158–167
30. Yang X, Liu C, Le Minh H, Wang Z, Chien A, Cheng KTT (2017) An automated method for accurate vessel segmentation. Physics in Medicine & Biology 62(9):3757
31. Zhang S, Chen W, Tang H, Han Q, Yan S, Zhang X, Chen Q, Parsons M, Wang S, Lou M (2016) The prognostic value of a four-dimensional ct angiography-based collateral grading scale for reperfusion therapy in acute ischemic stroke patients. PLoS One 11(8)